Sparing of tissue by using micro-slit-beam radiation therapy reduces neurotoxicity compared with broad-beam radiation therapy

Naritoshi Mukumoto[1], Masao Nakayama[1], Hiroaki Akasaka[1],
Yasuyuki Shimizu[1], Saki Osuga[1], Daisuke Miyawaki[1], Kenji Yoshida[1],
Yasuo Ejima[1], Yasushi Miura[2], Keiji Umetani[3], Takeshi Kondoh[4]
and Ryohei Sasaki[1]*

[1]Division of Radiation Oncology, Kobe University Graduate School of Medicine, 7-5-2 Kusunokicho, Chuouku, Kobe, Hyogo, 650-0017, Japan
[2]Department of Rehabilitation Science, Kobe University Graduate School of Health Sciences, Kobe, Hyogo, Japan
[3]Japan Synchrotron Radiation Research Institute, Sayo, Hyogo, Japan
[4]Department of Neurosurgery, Shinsuma Hospital, Kobe, Hyogo, Japan
*Corresponding author. Division of Radiation Oncology, Kobe University Graduate School of Medicine, 7-5-2 Kusunokicho, Chuouku, Kobe City, Hyogo, 650-0017, Japan. Tel: +81-78-382-6104; Fax: +81-78-382-6129; Email: rsasaki@med.kobe-u.ac.jp
Received March 16, 2016; Revised April 29, 2016; Accepted May 9, 2016

ABSTRACT

Micro-slit-beam radiation therapy (MRT) using synchrotron-generated X-ray beams allows for extremely high-dose irradiation. However, the toxicity of MRT in central nervous system (CNS) use is still unknown. To gather baseline toxicological data, we evaluated mortality in normal mice following CNS-targeted MRT. Male C57BL/6 J mice were head-fixed in a stereotaxic frame. Synchrotron X-ray-beam radiation was provided by the SPring-8 BL28B2 beam-line. For MRT, radiation was delivered to groups of mice in a 10×12 mm unidirectional array consisting of 25-µm-wide beams spaced 100, 200 or 300 µm apart; another group of mice received the equivalent broad-beam radiation therapy (BRT) for comparison. Peak and valley dose rates of the MRT were 120 and 0.7 Gy/s, respectively. Delivered doses were 96–960 Gy for MRT, and 24–120 Gy for BRT. Mortality was monitored for 90 days post-irradiation. Brain tissue was stained using hematoxylin and eosin to evaluate neural structure. Demyelination was evaluated by Klüver–Barrera staining. The LD_{50} and LD_{100} when using MRT were 600 Gy and 720 Gy, respectively, and when using BRT they were 80 Gy and 96 Gy, respectively. In MRT, mortality decreased as the center-to-center beam spacing increased from 100 µm to 300 µm. Cortical architecture was well preserved in MRT, whereas BRT induced various degrees of cerebral hemorrhage and demyelination. MRT was able to deliver extremely high doses of radiation, while still minimizing neuronal death. The valley doses, influenced by beam spacing and irradiated dose, could represent important survival factors for MRT.

KEYWORDS: microbeam, slit beam, synchrotron radiation, neurotoxicity, radiation therapy

INTRODUCTION

Micro-slit-beam radiation therapy (MRT) is a novel method of radiation therapy that involves irradiating tissue with arrays of parallel, narrow planes of synchrotron-generated X-rays [1–10]. The technique was first developed at the Brookhaven National Laboratory (Upton, NY, USA) [1, 2, 11] and the European Synchrotron Radiation Facilities (Grenoble, France) [12–14]. Laissue *et al.* [2, 13, 14] described surprisingly high tissue tolerances to multiple microbeams. In fact, tolerance was remarkably high even for developing tissues, which are well known to be radiosensitive. In MRT, highly directional and high-flux synchrotron radiation is spatially fractionated into quasi-parallel, microscopically thin, planar X-ray beams. Microbeams are usually reported to be 25–75 µm in width, with center-to-center (c-t-c) distances of 100–200 µm [1–3, 5–15].

Because MRT has only recently been developed, its mortality and toxicity with regard to irradiation of the central nervous system (CNS) has not yet been fully clarified. The tissue-sparing effect of X-ray microbeams was first evaluated by Slatkin *et al.* [1], who irradiated rat brains with synchrotron-generated planar microbeams. Their data demonstrated that there was no MRT-induced brain damage observed using 312–625 Gy entrance doses, even up to 4 weeks later; nor was there necrosis following entrance doses of between 312 and 5000 Gy [1]. To the best of our knowledge, there are no other reports evaluating mortality or neurotoxicity of MRT in normal (i.e. tumor-free) animals.

Extremely high-dose synchrotron beam irradiation can be generated using the 8 GeV beam of the SPring-8 facility. Since 2005, several studies using the SPring-8 synchrotron beam for MRT have been performed [16–19]. To further assess the toxicity of MRT, we evaluated mortality in normal mice after CNS-directed MRT.

MATERIALS AND METHODS
Micro-slit beam generation
These experiments utilized the BL28B2 beam-line of the SPring-8 synchrotron (Hyogo, Japan), the details of which are described in previous studies [17, 19]. Briefly, the beam-line provided an X-ray beam with a continuous energy spectrum mainly distributed between 50 and 200 keV, a critical energy of 28.9 keV, and a peak of around 90 keV. The calculated energy spectra have been reported previously [18]. The air kerma rate, measured using a free-air ionization chamber, has been determined to be 120 Gy/s at the peak and 0.7 Gy/s at the valley [19]. Doses delivered to the position where the animals were placed were 96–960 Gy for MRT, and 24–120 Gy for BRT. A slit-beam collimator consisting of two tungsten blocks was used to enable modulation of the variable microbeam width (Fig. 1a). A tantalum shutter upstream of the collimator controlled the beam pass and irradiation time. Radiation was localized by setting anterior–posterior windows and utilizing either a broad beam (as is used for broad-beam radiation therapy; BRT) or a 10 × 12 mm unidirectional array of microbeams (25 μm width and spacing of either 100, 200 or 300 μm) (Fig. 1b–d).

Evaluation of the dose in the phantom
For assessment of delivered doses of the microbeam, we employed Gafchromic dosimetry HD-V2 (Lot No. A03141301, ISP Technologies, Inc., Wayne, NJ) and EBT3 (Lot No. A12141101) films. The HD-V2 film had a dose range of 10–1000 Gy, which was appropriate for measuring the peak dose; the EBT3 film had a dose range of between 1 cGy and 40 Gy, which was appropriate for valley dose measurement. To read the optical density of the films, a microscope with bandpass filters (used to enhance the dose response on the reading system) and a charge-coupled-device (CCD) camera was used. Given the peak absorption spectra of HD-V2 and EBT3 are ~670 and ~585 nm, respectively, we chose bandpass filters with peaks of 670 nm and 585 nm, and full-widths at half-maximum (FWHM) of 13 nm and 17 nm, for reading the HD-V2 and EBT3 films, respectively. The Qicam Fast 1394 (Qimaging, Surrey, BC, Canada) CCD camera gave a resolution of 1392 × 1040 pixels, with a pixel size of 4.65 μm in a 12-bit grayscale digital output. The images were acquired at × 20 magnification with an exposure
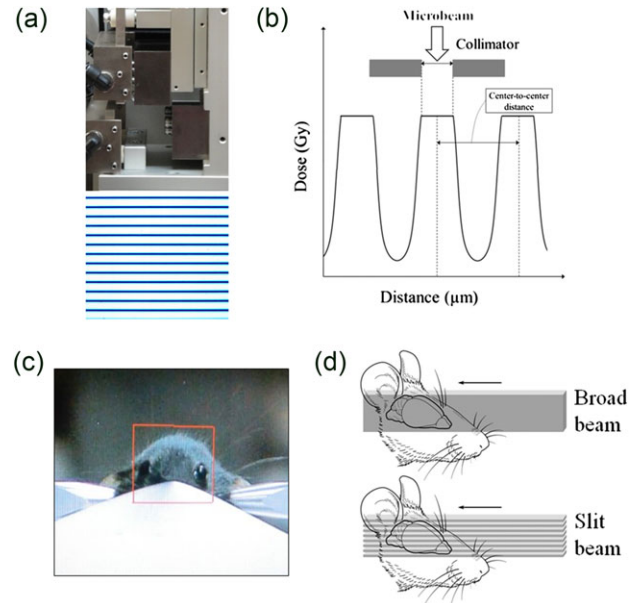

Fig. 1. Physical aspects of the experimental design. (a) A single-slit collimator which enables modulation of the peak width. Micro-slit beam dose distribution was confirmed using Gafchromic film. (b) Schematic view of the micro-slit beam dose profile in microbeam radiation therapy. (c) The total irradiation field of micro-slit beams from a 'beam's eye view'. The field size was about 12 mm wide and 10 mm high. (d) Schematic view of the irradiation geometry for broad and micro-slit beams.

time of 150 ms. Film was read ~24 h after irradiation, and analyzed using MetaMorph software version 6.2r6 (Molecular Devices, Sunnyvale, CA).

For testing, the films were inserted in a polymethylmethacrylate (PMMA) phantom, and microbeams with a 25-μm width and various c-t-c spacings were utilized to irradiate the phantom. The peak and valley doses at a depth of 1 cm in the phantom were evaluated. For dose evaluation, the films were irradiated in air, and the relationship between the radiation dose and the film optical density based on the known air kerma rate was determined. In the phantom study, the irradiation times of one microbeam for each film were determined by obtained calibration curves from previous assessments, and chosen so as to avoid film saturation. Each measurement was performed at least three times, and the mean values of these results were calculated.

MRT for animal experiments
Six-week old male C57/BL6J mice (*n* = 10 per group; CLEA Japan, Inc.) were used in this study. Each subject was completely anesthetized by intraperitoneal injection of pentobarbital sodium solution (6.48 mg/ml, 5–8 ml/kg), and then its head was secured in a fixed position via ear bars held in a stereotaxic frame (Narishige, Tokyo, Japan). Groups were monitored for mortality for 90 days after irradiation, and the mortality rate was plotted with Kaplan–Meier curves.

Immunohistochemical study

The mice that were evaluated for survival analyses after irradiation were carefully observed, and when a symptom believed to be caused by brain irradiation was noted, especially when subsequent

(a)

(b)

(c)

deterioration occurred, the affected mouse was humanely sacrificed with an anesthetic overdose. Mice that survived for the 4-week observation period were euthanized at that time. Thus, the calculated mortality rate would not be affected by the tissue collection. The brains to be prepared for immunohistochemical study were removed from the euthanized mice and processed as described below.

The brains were perfused with normal saline, and then with 50–70 ml of freshly prepared 4% paraformaldehyde (PFA). Each brain was then carefully removed and postfixed in 4% PFA solution. After removal, the brain was embedded in paraffin and sectioned coronally at 8 μm thickness (i.e. perpendicular to the plane of the microbeam). The brains were evaluated histologically for morphological changes using hematoxylin–eosin (H-E), and for demyelination via Klüver–Barrera staining.

All experimental protocols were approved by the animal welfare committees of the Japanese Synchrotron Radiation Research Institute SPring-8 (Permission No. 2013B1315 and 2012B1451) and by the Institutional Animal Care and Use Committee (Permission No. A110902); all protocols were carried out according to the Kobe University Animal Experimentation Regulations.

RESULTS
Peak and valley dose evaluation

We measured the peak and valley doses of microbeams with different center-to-center distances at a depth of 1 cm in the phantom. HD-V2 and EBT3 films were used for measurements of the peak (Fig. 2a) and valley (Fig. 2b) doses, respectively. The irradiating microbeam had a width of 25 μm, and the range of the beam spacing was between 50 and 300 μm. From the value of each peak dose and valley dose for the same center-to-center distance, the peak-to-valley dose ratio (PVDR) was calculated. The PVDR was essentially linear across the above-mentioned range (Fig. 2c).

Mortality

As shown in Fig. 3a, mortality within 90 days of using MRT (width/distance: 25/200 μm) was much lower than that for the same radiation dose using BRT. The LD_{50} and LD_{100} (50% and 100% lethal doses, respectively) using MRT were 600 Gy and 720 Gy, respectively, versus LD_{50} and LD_{100} doses of 80 Gy and 96 Gy, respectively, using BRT (Fig. 3a). Next, the mortality rates using MRT with various center-to-center distances were evaluated. Interestingly, mortality decreased with increasing center-to-center distances between 100 μm and 300 μm (Fig. 3b).
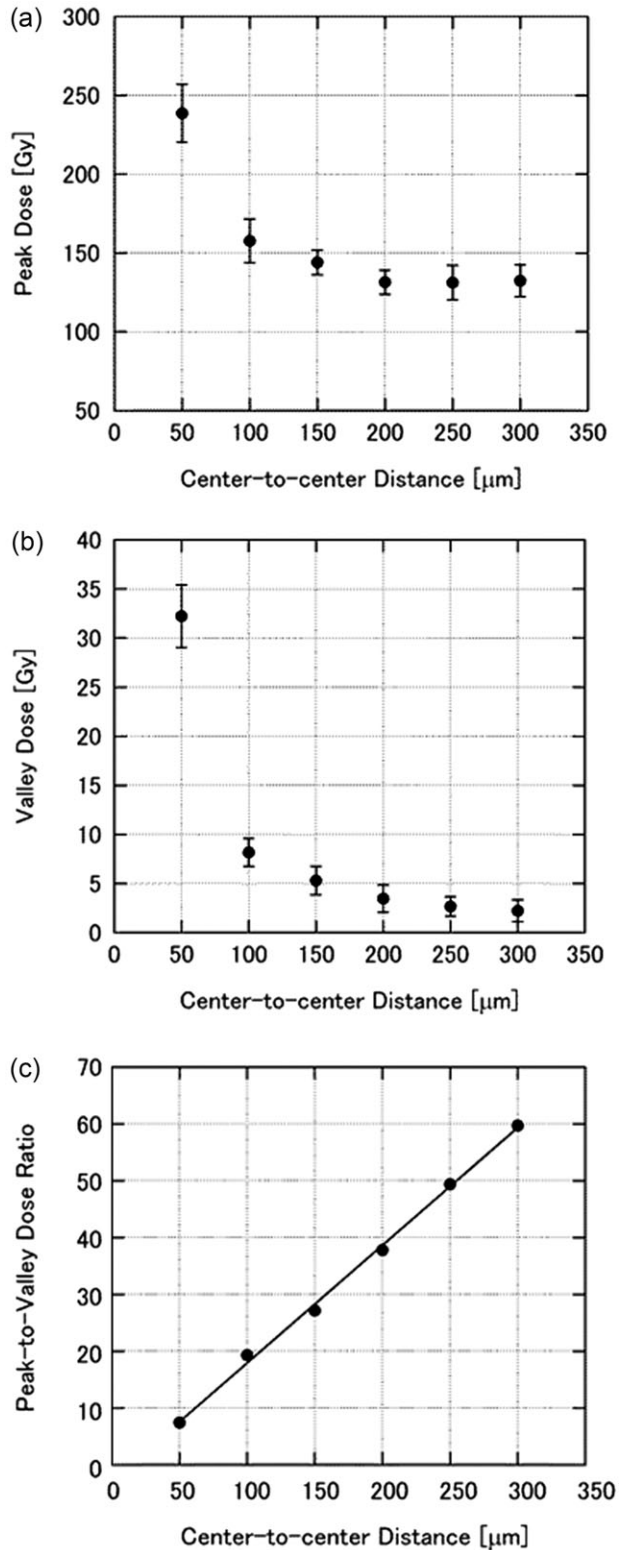
Fig. 2. The relationship between microbeam spacing and (a) peak dose, (b) valley dose, and (c) peak-to-valley dose ratio at a depth of 1 cm in a phantom. The microbeam width was 25 μm, and the spacing ranged from 50 μm to 300 μm. Peak and valley doses were measured using HD-V2 and EBT3 films, respectively. Each data point is the average of at least three measurements, and the error bars represent the standard deviation.
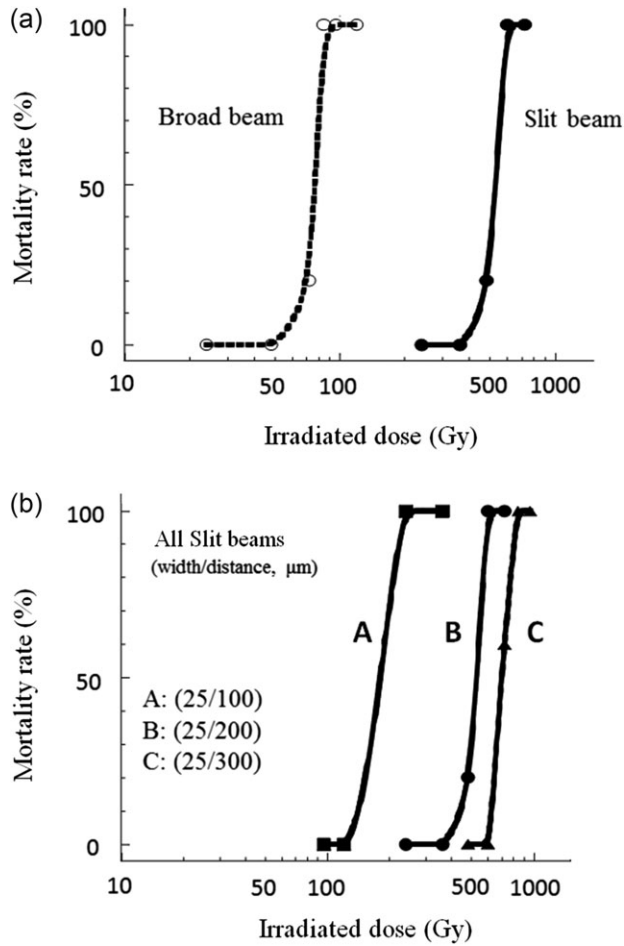
Fig. 3. Mortality results. (a) Mortality of mice observed for 90 days after whole brain irradiation via broad or micro-slit beams. (b) Comparison of mortalities using microbeam irradiation with different center-to-center distances (100–300 μm).

Survival duration

Survival durations after MRT or BRT were also evaluated. Using BRT, no mice survived for more than 20 days at doses of 84 Gy or 120 Gy (Fig. 4a). However, using MRT (width/distance: 25/200 μm), 80% of mice survived for 90 days at a dose of 480 Gy. Furthermore, no mice died at doses of 120 Gy or 360 Gy when using MRT (Fig. 4b). These data suggest that MRT was much less neurotoxic than BRT.

Cell loss and demyelination

The morphological effects of MRT (480 Gy) or BRT (120 Gy) were assessed using H-E and Klüver–Barrera staining (Fig. 5). After BRT, large numbers of neurons were lost, demyelination and partial cerebral hemorrhage were observed in the mice, and the maximum survival duration was 13 days (Fig. 5c and d). After MRT, neuronal cell loss corresponding to the micro-slit beams was observed without demyelination for the full 90 days (Fig. 5e and f). Cortical architecture was well preserved in MRT, whereas micro- or partial cerebral hemorrhage was seen in the specimens of the BRT group (Fig. 5c, d, e and f).

DISCUSSION

Radiation therapy plays a pivotal role in the treatment of many CNS tumors; however, whole-brain irradiation or partial high-dose irradiation (i.e. radiosurgery) can have adverse effects on normal brain tissue. Shibamoto *et al.* demonstrated that brain atrophy developed in up to 30% of patients after whole-brain irradiation (40 Gy in 20 fractions), but they also noted that it was not necessarily accompanied by mini-mental state examination (MMSE) score decreases [20]. Radiosurgery delivers higher doses (15–20 Gy in a single fraction) better localized to the tumors, though this method might cause radiation necrosis, a severe and irreversible complication. Multiple retrospective studies have reported rates of radiation necrosis ranging from 14% to 24% [21, 22]. Those studies determined that the rate of radiation necrosis was largely dependent upon the radiation dose and the irradiated volumes. Interestingly, although our use of MRT delivered over 10-fold more radiation than radiosurgery, MRT still did not induce radiation necrosis. This
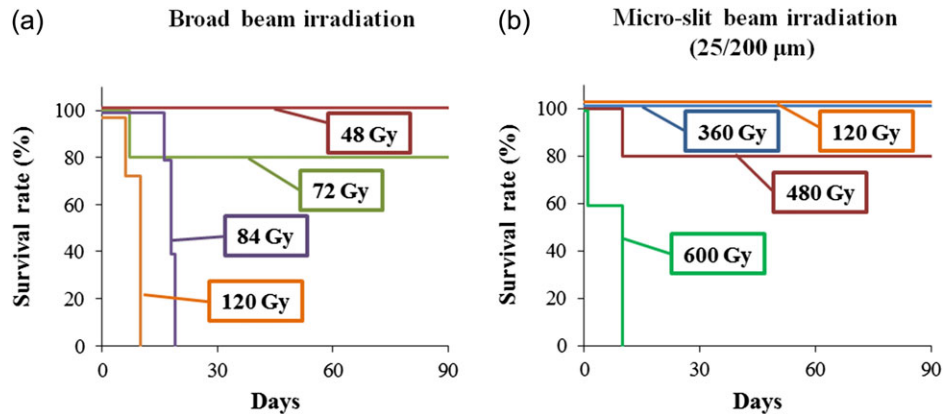

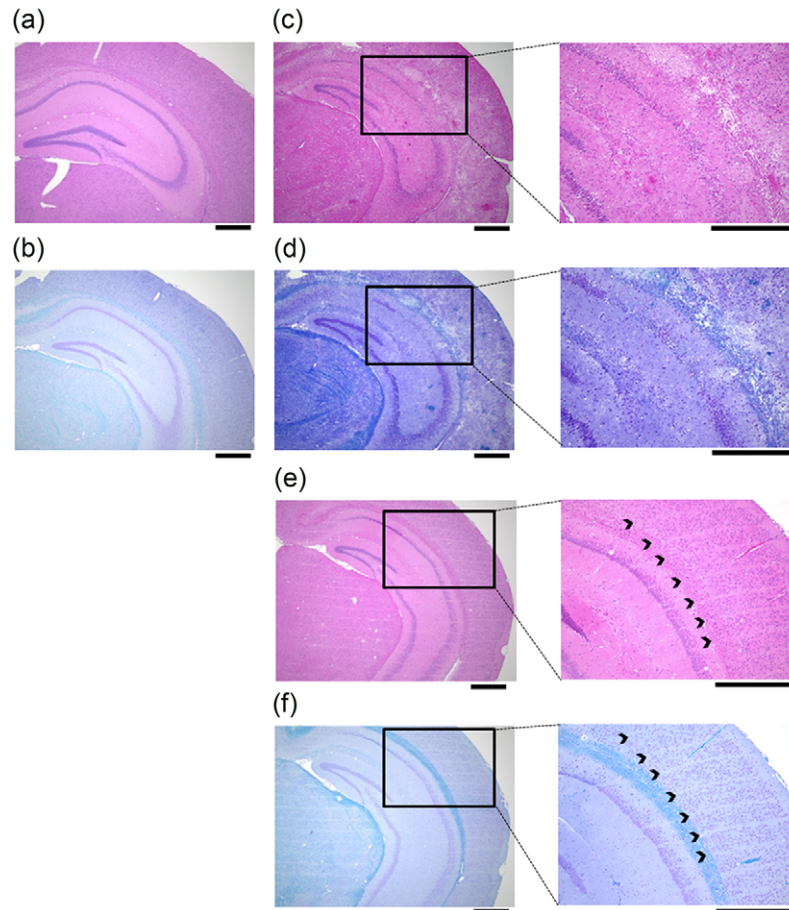Fig. 4. Survival durations following broadbeam and microbeam irradiation plotted on Kaplan–Meier graphs.

Fig. 5. Histological analysis of cortical structure. Representative hematoxylin-eosin and Klüver-Barrera staining in (a, b) control sections; (c, d) sections taken 13 days after irradiation with a 120 Gy broadbeam; and (e, f) sections taken 90 days after irradiation with a 480 Gy micro-slit beam. All scale bars = 500 μm.

point alone seems to be a strong advantage of MRT over the previously mentioned radiation techniques.

Reduction of mortality, preservation of cortical architecture, and inducing factors following high-dose MRT are goals creating great interest in the development of novel experimental models in neurobiology. Unidirectional irradiation using microbeam arrays has confirmed the exceptional resistance of normal tissue to high doses of radiation in MRT [3–6, 10, 23], a radiobiological phenomenon referred to as the 'tissue-sparing effect'. This effect describes the preservation of the architecture of the tissues post irradiation. Multiple studies have demonstrated that the doses delivered to cells and tissues between the microbeams (the 'valley' doses) are probably the most important determinants of normal tissue damage in MRT [2, 4, 14, 23, 24]. For a given target, the valley dose depends on three main parameters: the microbeam width, the spacing between the microbeams, and the dose delivered along each microbeam. We showed that increasing the center-to-center space between the microbeams clearly improved survival of the irradiated mice (Fig. 3b). If the valley dose is reduced by increasing spacing between the microbeams, as would be expected, our data indicate that the center-to center space is a very important parameter for

survival, at least in mice. The delivered dose was also found to be critically important, given the differences in mortality we saw when changing dose, but not beam width or distance (Fig. 3b). Not only are our data consistent with the previously reported findings, but they have clarified the relative importance of center-to-center beam distance and irradiated dose, both of which directly influence valley dose, as important and useful determinants of mortality in MRT. Because the valley dose is so difficult to measure accurately *in vivo*, measurements using phantoms or calculated values are important.

Assessments related to the valley dose or the PVDR are central to the understanding of MRT. Many studies have employed film measurements and/or Monte Carlo calculations for MRT dosimetry [18, 19, 24, 25]. Although film measurement is often used for MRT dosimetry because of its spatial resolution and convenience, it is noteworthy that errors in film measurement might be generated by several factors, including sensitivity differences, density–dose conversion curves, and reading procedures or conditions. For instance, we used two Gafchromic films with different sensitivities, bandpass filters, and a CCD camera for reading films. Crosbie *et al.* [24] used the same beamline as this study, two films (HD810, range: 10–400 Gy; EBT range: 0.01–8 Gy) and a microdensitometer. Their results

indicated that the PVDR at 10-mm depth was ~67 for microbeams with a beam width of 25 μm and a center-to-center spacing of 200 μm. As shown in Fig. 2, the PVDR in our data was 39 under the same conditions, and was slightly lower than that reported by Crosbie [24]. This difference might be related to the procedure for reading the valley dose, given our use of similar films. Monte Carlo simulation is believed to be useful in calculating the theoretical dosimetric values in MRT, although reports have found discrepancies between the measured and calculated valley doses [19, 24]. In terms of the PVDR of a beam width of 25 μm and a center-to-center spacing of 200 μm, the values calculated by Monte Carlo simulation ranged from 29 to 53 in the 0–1 cm depth in previous studies [7, 11, 26, 27]. Thus, the methods of measurement and calculation of the MRT are still matters of debate, and more data or reports seem to be necessary to determine the best practices for MRT.

Radiation-induced vascular damage considerably influences the overall cerebral response to radiotherapy [28]. Vascular necrosis induces late, progressive and often irreversible changes in cerebral tissue. Macroscopically, MRT avoids radiation necrosis and preserves the architecture of the irradiated tissue, phenomena attributed mainly to the rapid regeneration of normal microvessels. Only a short segment of the microvascular bed receives an ablative dose, while the adjacent endothelial cells in the region around the valley dose receive just a few Grays, allowing for continuity of the vascular supply [5, 18, 23]. The natural repair of the normal microvasculature by migration of unaffected cells surrounding the microbeam paths is believed to be the mechanism underlying the high dose tolerance of normal tissue seen in MRT [8, 29]. Serduc et al. [29] published data from a glioma-bearing mouse model indicating that the mechanism of action of MRT did not involve a significant microvascular component. They postulated that tumor cell reduction, rather than a failure of endothelial cells to repair vessels, might be the principal mechanism in their mouse brain tumor model.

In conclusion, MRT is advantageous for delivering extremely high doses of radiation, while still preserving cortical architecture and minimizing neuronal death (and mortality). The valley doses, influenced by beam spacing and delivered dose, may be relatively important survival factors.

ACKNOWLEDGEMENTS

FUNDING

CONFLICT OF INTEREST
There is no conflict of interest for any of the authors.

REFERENCES

1. Slatkin DN, Spanne P, Dilmanian FA, et al. Subacute neuropathological effects of microplanar beams of x-rays from a synchrotron wiggler. *Proc Natl Acad Sci USA* 1995;92:8783–7.
2. Laissue JA, Geiser G, Spanne PO, et al. Neuropathology of ablation of rat gliosarcomas and contiguous brain tissues using a microplanar beam of synchrotron-wiggler-generated X rays. *Int J Cancer* 1998;78:654–60.
3. Dilmanian FA, Button TM, Le Duc G, et al. Response of the rat intracranial 9L gliosarcoma to Microbeam Radiation Therapy (MRT). *Neuro-Oncol* 2002;4:26–38.
4. Dilmanian FA, Morris GM, Zhong N, et al. Murine EMT-6 carcinoma: high therapeutic efficacy of microbeam radiation therapy. *Radiat Res* 2003;159:632–41.
5. Blattmann H, Gebbers J-O, Bräuer-Krisch E, et al. Applications of synchrotron X-rays to radiotherapy. *Nucl Instrum Methods Phys Res A* 2005;548:17–22.
6. Dilmanian FA, Qu Y, Liu S, et al. X-ray microbeams: tumor therapy and central nervous system research. *Nucl Instrum Methods Phys Res A* 2005;548:30–7.
7. Bräuer-Krisch E, Requardt H, Régnard P, et al. New irradiation geometry for microbeam radiation therapy. *Phys Med Biol* 2005;50:3103–11.
8. Serduc R, Vérant P, Vial JC, et al. In vivo two-photon microscopy study of short-term effects of microbeam irradiation on normal mouse brain microvasculature. *Int J Radiat Oncol Biol Phys* 2006;64:1519–27.
9. Smilowitz HM, Blattmann H, Bräuer-Krisch E, et al. Synergy of gene-mediated immunoprophylaxis and microbeam radiation therapy for advanced intracerebral rat 9L gliosarcomas. *J Neuro-oncol* 2006;78:135–43.
10. Dilmanian FA, Zhong Z, Bacarian, et al. Interlaced x-ray microplanar beams: a radiosurgery approach with clinical potential. *Proc Natl Acad Sci USA* 2006;103:9709–14.
11. Slatkin DN, Spanne P, Dilmanian FA, et al. Microbeam radiation therapy. *Med Phys* 1992;19:1395–400.
12. Thomlinson W, Berkvens P, Berruyer G, et al. Research at the European synchrotron radiation facility medical beamline. *Cell Mol Biol* 2000;46:1053–63.
13. Laissue JA, Lyubimova N, Wagner HP, et al. Microbeam Radiation Therapy. *Proc SPIE* 1999;3770:38–45.
14. Laissue JA, Blattmann H, Di Michiel M, et al. The weanling piglet cerebellum: a surrogate for tolerance to MRT (microbeam radiationtherapy) in pediatric neuro-oncology. *Proc SPIE* 2001;4508:65–73.
15. Serduc R, Bräuer-Krisch E, Bouchet A, et al. First trial of spatial and temporal fractionations of the delivered dose using synchrotron microbeam radiation therapy. *J Synchrotron Radiat* 2009; 16:587–90.

16. Crosbie JC, Anderson RL, Rothkamm K, et al. Tumor Cell Response to Synchrotron Microbeam Radiation Therapy Differs Markedly From Cells in Normal Tissues. *Int J Radiat Oncol Biol Phys* 2010;77:886–94.

17. Uyama A, Kondoh T, Nariyama N, et al. A narrow microbeam is more effective for tumor growth suppression than a wide microbeam: an *in vivo* study using implanted human glioma cells. *J Synchrotron Radiat* 2011;18:671–8.

18. Ohno Y, Torikoshi M, Suzuki M, et al. Dose distribution of a 125 keV mean energy microplanar x-ray beam for basic studies on microbeam radiotherapy. *Med Phys* 2008;35:3252–8.

19. Nariyama N, Ohigashi T, Umetani K, et al. Spectromicroscopic film dosimetry for high-energy microbeam from synchrotron radiation. *Appl Radiat Isot* 2009;67:155–9.

20. Shibamoto Y, Baba F, Oda K, et al. Incidence of brain atrophy and decline in mini-mental state examination score after whole-brain radiotherapy in patients with brain metastases: a prospective study. *Int J Radiat Oncol Biol Phys* 2008;72:1168–73.

21. Blonigen BJ, Steinmetz RD, Levin L, et al. Irradiated Volume as a Predictor of Brain Radionecrosis After Linear Accelerator Stereotactic Radiosurgery. *Int J Radiat Oncol Biol Phys* 2010;77:996–1001.

22. Minniti G, Clarke E, Lanzetta G, et al. Stereotactic radiosurgery for brain metastases: analysis of outcome and risk of brain radionecrosis. *Radiat Oncol* 2011;6:48.

23. Romanelli P, Bravin A. Synchrotron-generated microbeam radiosurgery a new experimental approach to modulate brain function, *Neurol Res* 2011;33:825–31.

24. Crosbie JC, Svalbe I, Midgley SM, et al. A method of dosimetry for synchrotron microbeam radiation therapy using radiochromic films of different sensitivity. *Phys Med Biol* 2008;53:6861–77.

25. Shinohara K, Kondoh T, Nariyama N, et al. Optimization of X-ray microplanar beam radiation therapy for deep-seated tumors by a simulation study. *J Xray Sci Technol* 2014;22:395–406.

26. Stepanek J, Blattmann H, Laissue JA, et al. Physics study of microbeam radiation therapy with PSI-version of Monte Carlo code GEANT as a new computational tool. *Med Phys* 2000;27:1664–75.

27. Siegbahn EA, Stepanek J, Brauer-Krisch E, et al. Determination of dosimetrical quantities used in microbeam radiation therapy (MRT) with Monte Carlo simulations. *Med Phys* 2006;33:3248–59.

28. Schultheiss TE, Kun LE, Ang KK, et al. Radiation response of the central nervous system. *Int J Radiat Oncol Biol Phys* 1995;31:1093–112.

29. Serduc R, Christen T, Laissue J, et al. Brain tumor vessel response to synchrotron microbeam radiation therapy: a short-term in vivo study. *Phys Med Biol* 2008;53:3609–22.